A Novel SPEEK-PVA-TiO_2 Proton Conducting Composite Membrane for PEMFC Operations at Elevated Temperature

RABIRANJAN MURMU[1*] AND HAREKRUSHNA SUTAR[1,2]

[1]*Chemical Engineering Department, Indira Gandhi Institute of Technology Sarang, Odisha, India.*
[2]*Chemical Engineering Department, Jadavpur University, Kolkata, India.*

ABSTRACT

A novel Sulfonated polyether etherketone (SPEEK) - Polyvinyl alcohol (PVA) -Titanium dioxide (TiO_2) composite membrane is prepared for proton exchange membrane fuel cell (PEMFC) by solution casting method. In order to enhance the mechanical, thermal and hydrolytic stability of the SPEEK/PVA film; different compositions of TiO_2 particles are dispersed as filler. Membrane uniformity is confirmed by Scanning Electron Microscopy (SEM). Composite membrane is characterized by FTIR, XRD, water uptake, Ion Exchange Capacity (IEC), DSC, TGA and Proton conductivity. Prepared composite membrane shows better water uptake capacity with lowering IEC. TiO_2 has the significant effect on methanol permeability of the composite membrane. The prepared composite membrane provides good thermal, mechanical and hydrolytic stability at higher temperature (above 80°C) due to the strong intermolecular attraction between TiO_2 and polymer backbone. At above 80°C, lightly cross linked SPEEK/PVA/TiO_2 composite provides superior proton conductivity than SPEEK membrane due to strong hydrogen bonding between TiO_2 and water resulting reduction of water loss. Proton conductivity result shows linear improvement for SPEEK/PVA membrane by dispersing TiO_2 and the data ranges in the order of 10^{-5} S/cm at 30°C to 10^{-1} S/cm at 110°C. But at lower temperature, SPEEK/PVA/TiO_2 composite provide poor proton conductivity due to lower IEC and DS.

KEY WORDS : *PEMFC, SPEEK, Diffusivity, Proton Conductivity*

J. Polym. Mater. Vol. **35,** No. 4, 2018, 409-431

Correspondence author e-mail : rabiranjan_murmu@rediffmail.com, h.k.sutar@gmail.com
DOI : https://doi.org/10.32381/JPM.2018.35.04.2

1. INTRODUCTION

Now days, the demand of petroleum based energy resource gradually increases. But due to its limited availability, high toxic emission and adverse effect to the environment, forced us to development of potential alternatives [1]. In recent year, fuel cell technology received more attention because of its high efficiency and lower toxic emission. Fuel cell is a device that continuously converts the chemical energy from a fuel like hydrogen, methanol etc. into electricity through an electro chemical reaction [2]. PEMFC is an efficient electro chemical conversion device for stationary and portable applications. In PEMFC, a proton conducting polymer is used as an electrolytes [3-5]. In PEMFC, proton transport plays a vital role for achieving more power density [6, 7]. Proton exchange membrane (PEM) is one of the important components of a PEMFC for achieving high power density. It is a selective permeable membrane which allows the transport of protons from anode side to cathode side and separate reactant gases from each other. For achieving high power density, PEM should have better proton conductivity, low reactant permeability, excellent electron insulation property, low cost, easily prepared, better mechanical, thermal and hydrolytic stability. Perfluorinated sulfonic acid membranes (PFSA) like Nafion (Dupont®) are considered as a conventional PEM membrane because of their high proton conductivity, good mechanical and thermal stability at low temperatures [5,8]. But their applications are restricted because of their high cost, low proton/vanadium ion selectivity, poor mechanical properties at swollen condition and dramatic reduction of proton conductivity above 80°C. Poor performance at higher temperatures is due to the loss of water by evaporation, high fuel cross over, poor thermal stability and possibility of environment contamination. [8-10].

Now SPEEK is widely considered as a potential alternative of Nafion because of its low methanol permeability, good thermal stability, easily prepared, low cost and provides good proton conductivity. Proton conductivity of the SPEEK membranes is studied at various temperature [11-14] and humidity [15]. Study reveals that the water uptake has greatest effect on proton conductivity [16]. But the physical and chemical properties of the membranes are highly influenced by degree of sulfonation (DS) [16]. With increase in DS, proton conductivity rises, but because of its high swelling ability leads to poor mechanical property [17]. Degree of sulfonation improves the properties of SPEEK membrane at certain extent, but that is not enough for PEMFC applications due to its poor mechanical properties and thermal stability. With increase in temperatures (above 85°C), proton conductivity drastically decreases due to poor water retention capacity [37]. To improve the properties of SPEEK membranes, several attempts have been made like cross linking [18-22], ionic liquid composites [23] and nanoparticle incorporation. PVA is considered as a potential alternative membrane in fuel cell due its good proton conductivity because of more hydrophilic domain and low methanol permeability [24]. To reduce methanol crossover and improve proton conductivity, PVA is blended with conventional Nafion membrane [25, 26]. Study reveals that the proton conductivity decreases with increase of PVA content in the composite [27]. It was found that the blend of SPEEK/PVA provide better

conductivity at low water uptake due to enriched hydrophilic domain. But its performance decreases at high temperature due to its poor water retention capacity and thermal stability. Due to the presence of more hydrophilic domain, membrane swells more resulting poor mechanical stability [28]. Study reveals that the used of cross-linked PVA/TiO_2 composite membranes provide better electrochemical performance at a specified condition [29].

The dispersion of ceramic filler into the base polymer reduces glass transition temperature (T_g) and crystallinity of the polymer composite. The polymer composites become more amorphous and allow better ionic conductivity. For improving water retention capacity and thermal stability at higher temperature (above 80°C), several researchers have studied the effect of inorganic metal oxides on SPEEK membrane [30, 31, 32]. The selection of hygroscopic material as a ceramic filler is best option for maintaining high water retention capacity. There are various hygroscopic materials, such as Al_2O_3, TiO_2 [33], SiO_2 [34], ZrO_2 [35] have been extensively studied. The study reveals that the use of ceramic filler in a SPEEK membrane provide better proton conductivity due to more water retention capacity with lower IEC and provide better thermal stability [35]. The SPEEK membrane incorporated with graphene oxide (GO) provide better proton conductivity with high mechanical, thermal and hydrolytic stability[36]. Although the composite membranes provide better conducting than SPEEK membrane but performance above 80°C is not studied till date. Due to high cost of graphene oxide forced us to development of composite membrane focusing on low cost with excellent mechanical, thermal and hydrolytic stability.

In this work, we attempted to disperse the nano-sized TiO_2 particles into the SPEEK/PVA matrix to produce comparatively cheaper proton exchange membrane for medium to higher temperature PEMFC application. The homogeneous composite membranes were prepared by solution casting method. The TiO_2 particle was well distributed in a composite by proper mixing. The effect of different loading of TiO_2 (0-12 wt %) on SPEEK membranes were investigated focusing on different stability features. The Physicochemical and electrochemical characteristics of prepared composite membranes were investigated and compared with plain SPEEK and SPEEK/PVA membrane. The water uptake behavior, TGA, DSC, SEM, tensile stress-strain test, IEC, proton conductivity and hydrolytic stability were studied.

2. EXPERIMENTAL

2.1 Materials

Bulk quantity of Poly Ether Ether Ketone (PEEK) powder with mean particle size 80 micron was purchased from Sigma Aldrich, Bangalore. Polyvinyl Alcohol, sulfuric acid (98% conc.) and titanium dioxide was purchased from local chemical supplier Talcher, Odisha. Dimethyl Acetamide as a solvent was purchased from Sigma Aldrich, Bangalore. Hydrochloric acid, sodium chloride, sodium hydroxide and phenolphthalein indicator used for titration was availed in our laboratory.

2.2 Membrane Preparation

PEEK powder (7 wt%/vol. of H_2SO_4) was mixed in a sulfuric acid for 3 hour reaction time at 60°C by using preset magnetic stirrer rotating at 600 rpm. After reaction was completed, the sulfonated solution was poured into distilled water by using burette. The polymer bead obtained by this process was further washed with distilled water for several times to make it slightly acidic. The preparation of SPEEK granules from PEEK powder is mentioned in our earlier research [37]. After

confirming the degree of sulfonation (DS) of the SPEEK granules by adopting titration method, the SPEEK granules were used for composite preparation. SPEEK granules and Polyvinyl alcohol (70/30 wt%) were mixed properly by the medium of Dimethyl acetamide solvent in a digital magnetic stirrer with proper agitation for 2 hour at 60°C. After uniform mixing, different content of Titanium dioxide (4%, 8% and 12%) was uniformly dispersed by sonicator to prepare different composition of composite membrane. After dispersion, the solution was further mixed thoroughly in a magnetic stirrer for 2 hour at 600 rpm. Then the solution mixture was poured into a Petri disc and kept at open atmosphere for 12 hours. Further reduction of moisture and volatile solvent was attained by treating in a hot air oven at 60°C for 24 hours followed by 12 hour at 80°C. During drying, moisture and volatile solvent is evaporated resulting thin sheet of film on the surface of Petri disc. After drying, thin sheet of film was peeled off from the Petri disc by adding little amount of water. The composite membrane obtained by this method has the film thickness of 120 µm. Now composite membrane is ready for analysis.

2.3 Ion Exchange Capacity and Degree of Sulfonation

Ion exchange capacity of the composite membrane was measured by standard titration method. Composites membrane with film thickness 120µm, were cut into circular shape (surface area: 11.342 cm^2) by using die cutting machine. Before testing, sample was dried in a hot air oven for 30 minutes at 60°C. Dry Sample was immersed in a 0.1M of Hydrochloric acid for 24 hour to ensure H^+ ion transport. After protonation, surface of membrane was washed with distilled water till there is no free proton present on it. Then acidified membrane is immersed in a 0.1M of NaCl solution for exchange of proton (H^+) with Na^+ ions. The IEC is measured by the following expression

$$\text{IEC (meqg}^{-1}) = \frac{V_{NaOH}\, C_{NaOH}}{W_d} \quad (1)$$

V_{NaOH} is the volume (ml) of NaOH consumed by titration, C_{NaOH} is the concentration (mol/l) of NaOH used for titration and W_d is the weight (gm) of dry membrane.

DS of the pure SPEEK is calculated by following expression

$$\text{DS} = \frac{M_{SPEEK} \times IEC}{1-(IEC \times M_{SO_3H})} \times 100 \quad (2)$$

M_{SPEEK} is the molecular weight (288) of SPEEK without functional group, M_{SO_3H} is the molecular weight (81) of sulfonic group present in SPEEK and IEC is in $meqg^{-1}$. IEC and DS of the all composite membrane were determined by using equation-1 and 2.

2.4 Water uptake and Diffusivity

Before water uptake study; composite membrane was dried in a hot air oven for 30 minute at 60°C. Dry weight of the membrane was measured by a digital balance and noted. Then dry membrane is immersed in distilled water till equilibrium weight of the membrane achieved. During absorption process, at a particular interval of time membrane is kept out from the container and surface water is cleaned properly by tissue paper. Then immediately weight of wet membrane is taken. The above procedure is continued for different interval of time till membrane achieved equilibrium value. Water uptake capacity of the different composite membrane was measured at different temperature. Water uptake capacity (WU) is measured by using following expression

$$WU\ (\%) = \frac{W_{wet} - W_{dry}}{W_{wet}} \quad (3)$$

W_{wet} is the equilibrium weight (gm) of the membrane and W_{dry} is the dry weight (gm) of the membrane. The number of water molecule absorbed per sufonate group ($-SO_3H$ group) present in composite membrane is calculated by using following expression [35].

$$\lambda = \frac{10 \times WU}{IEC \times MW_{H_2O}} \quad (4)$$

Where λ is the number of water molecule absorbed per sulfonate (SO_3^-) group, WU is the water uptake capacity (%), IEC is the ion exchange capacity ($meqg^{-1}$) and MW_{H_2O} is molecular weight of water (18 $gmmol^{-1}$). Experimental λ value for different composite membrane at different temperature is determined by using equation-4.

The rate of water absorption in the membrane is controlled by diffusion. The behavior of water diffusion was well explained by Fickian diffusion. Several Fickian model was proposed by different researchers for measuring water diffusivity but the model proposed by Takamatsu et al. [38] and Morris and Sun [39] is more effective for analysis. The model equation used for measuring water diffusivity is

$$\frac{M_t}{M_\infty} = \exp(-kt) \quad (5)$$

M_t is the water uptake at time t, M_∞ is the equilibrium water uptake, k is the effective rate constant and t is the duration of time. By plotting moisture ratio (M_t/M_∞) with time, slope of the curve provides effective rate constant, k. After estimating k, diffusivity value is calculated by using following expression

$$D\ (cm^2/s) = kL^2 \quad (6)$$

D is the water diffusivity, cm^2/s and L is the thickness of membrane. The water uptake study is performed at different temperature and at a particular temperature; diffusivity is measured by using equation-5 and 6.

2.5 Methanol Permeability

Methanol permeability (P) of the composite membrane was determined by using a glass diffusion cell separated by two compartments. One compartment filled with methanol concentration are called donor reservoir and the other compartment which was initially filled up with deionized water are called receiver reservoir. The composite membrane was sandwiched between the two compartments. Before performing test, proper hydration of the composite membrane was obtained by immersing it in distilled water for 24 hours. The methanol transported through the composite membrane into water compartment was measured at a regular interval of time using a density meter (model: DA-130N, Kyoto Electronics Manufacturing Co., Ltd., Kyoto, Japan). At a particular interval of time, 0.25 ml of sample was collected from the receiver compartment and weighed. Then concentration of solution was determined by density meter. During experiment both compartments were agitated continuously. The methanol permeability (P) was calculated from following equation

$$C_B = \frac{A}{V}\frac{DK}{L} C_A\ (t-t_0) \quad (7)$$

Here C_B and C_A are the concentration of methanol in water and methanol compartment (mol L^{-1}) respectively; L is the thickness of the membranes (cm), A is the effective diffusion area (cm^2) and V is the volume of deionized water in water compartment (mL), D is the methanol diffusivity (cm^2s^{-1}), K is the partition coefficient between membrane and solution, t is the duration time (minute) and t_0 is the time lag, related to diffusivity as $t_0 = \frac{L^2}{6D}$. The product "**DK**" is called membrane permeability in cm^2s^{-1}. Methanol permeability is obtained from the slope of curve plotted between permeated methanol concentrations with time.

3. Membrane Characterization

3.1 Scanning Electron Microscopy (SEM)

A different composite membrane surface was well captured by SEM (JEOL; JSM-6480 LV, Japan). Uniformity of the composite membrane is confirmed by SEM images. Before performing SEM test, membrane is chopped into small size. Before performing test, membrane cross section was sputtered with thin layer of gold. Different SEM images were taken for composite membrane at the range of 200-9000 magnification. Dispersion of titanium dioxide particle and its size in a composite is well recognized from the SEM image at high resolution (3000-9000 magnification).

3.2 Fourier Transform Infrared Spectroscopy (FTIR)

FTIR of the sample is conducted to find the different functional groups present in it. Particular thickness of dry sample is cut into small piece and kept it in a FTIR machine. Infra red light is passed in the sample and intensity of light is measured in the wavelength range of 400-4000cm^{-1}. Different function group of composite is observed due to appearance of the characteristic peak at different wavelength region.

3.3 X-ray Diffraction (XRD) analysis

XRD technique is used to identify the phase of crystalline material. Finely ground sample is analyzed by X-ray Diffractometer (Philips, PW1720, USA). Composite membrane is dried and grounded into powder form and

placed into the sample holder of machine. X-ray incident light produced by Cu Kα radiation at 40 kV and 30 mA is passed to the sample and scanning is done at different diffraction angle (2θ) ranges between 10-90°.

3.4 DSC and TGA analysis

The change of the state of the composite membranes with action of heat is studied by DSC (Perkin-Elmer DSC7, MA, USA). Composite membrane is cut into small size and approximately 5 mg of sample is used for analysis. The sample is heated from 29-300°C under nitrogen atmosphere with fixed heating rate of 10°C/min. The experiment is performed with two heating cycle and one cooling cycle for each sample.

The thermal stability of the composite membranes is studied by TGA (Perkin-Elmer TGA, MA, USA). For analysis, 10 mg of sample is used. The sample is heated from 29-800°C under nitrogen atmosphere with fixed heating rate of 10°C/min.

3.5 Hydrolytic stability

The composite membrane is initially dried at 60°C for 2 hour and dry weight of the membrane is measured. Then the sample is submerged in distilled water for one day till equilibrium value achieved. Under equilibrium condition, membrane becomes saturated and that will not absorb water. Then weight of the membrane is measured and kept it in a controlled humidity chamber (RH-78%, 29°C) for 6 days. The rate of weight loss with time is studied focusing on hydrolytic stability. For a particular interval of time, weight of the membrane is measured and the procedure is continued for 6 days.

3.6 Proton conductivity

Proton conductivity of the composite membrane between 30-110°C was studied by two probe method electrochemical impedance spectroscopy (EIS) using a potentiostat (Biologic, SP-150) using the frequency range of 1 to 3×10^6 Hz, applying oscillation voltage amplitude of 10 mV. Before performing test, membrane is fully hydrated by immersing in distilled water for 24 hour. The hydrated membrane is sandwiched between two electrodes and constant electric voltage was supplied. The thickness of the hydrated membrane was measured by screw gauge. The proton conductivity of the sample is calculated by using the following equation

$$\sigma = \frac{L}{R_b A} \tag{8}$$

Here, σ is proton conductivity (Scm^{-1}), R_b is bulk resistance (ohm) and A is effective area of sample sandwiched between two electrodes during measurement and L is the thickness of membrane (cm). Bulk resistance (R_b) can be obtained at the low intersect of high frequency semicircle region from the complex impedance (Re_Z) plane. Proton conductivity is obtained by two methods: (1) from the Bode plot, (2) from the Nyquist plot.

3.7 Mechanical stability

Mechanical stability of the composite membrane is studied by Universal Testing Machine (UTM3382, Instron, UK). For analysis, Samples were prepared based on ASTM standard (D882-01). The sample is cut into rectangular shape of 2cm × 8cm and the tensile rate is fixed at 10 mm/min.

4. RESULTS AND DISCUSSION

SEM cross sectional image of different polymer composite at different magnifications is shown in fig. 1. Membrane uniformity of the pure SPEEK membrane is clearly observed in fig. 1(a). The sulfonate group present in the SPEEK sample is well attached in the PEEK backbone. Morphology confirms the homogeneity of structure with defect free. But incorporating different composition (4, 8 and 12%) of TiO_2 particles in the SPEEK/PVA matrix, composite surface becomes rough and heterogeneity in structure. Non homogeneity of the structure is well observed in fig. 1(b, c, d). The uniform distribution of TiO_2 in SPEEK/PVA composite is observed for 4 and 8% TiO_2 loaded composites. The uniformity of TiO_2 in SPEEK/PVA composites are shown in fig. 1(b,c). Further addition of TiO_2 (12%), composite becomes bulky dense microstructure with

randomly distributed TiO_2. The TiO_2 aggregates with each other to form cluster creating huge defect in a composite. The aggregation of TiO_2 particles in SPEEK/PVA composite is shown in fig. 1(c). Different sizes of TiO_2 agglomerated in a composite membrane are clearly observed from the SEM image taken at 8000 magnification.

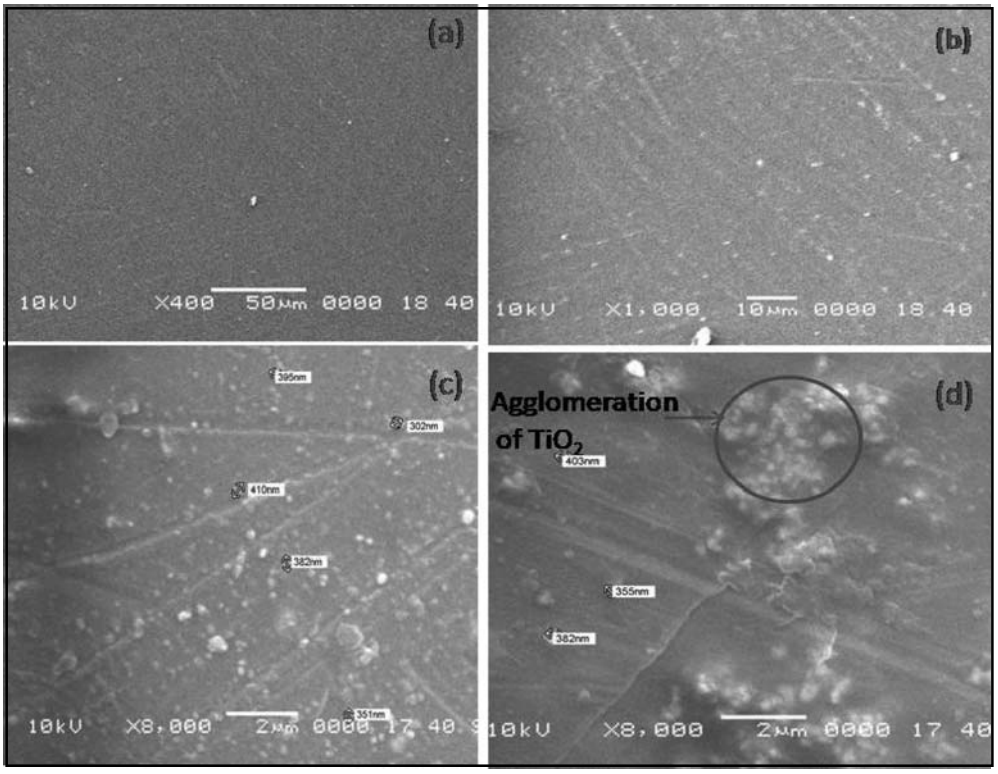

Fig. 1. Cross sectional SEM image of (a) Pure SPEEK (b) SPEEK/PVA-4% TiO_2 (c) SPEEK/PVA-8% TiO_2 (d) SPEEK/PVA-12% TiO_2

Different functional group present in composite membrane is shown in fig. 2. Prominent peak observed for all composite at 723 cm^{-1} is due to Ti-O bending (from TiO_2). The prominent peak at 630, 1100 and 1660 cm^{-1} is attributed to PEEK. Broad peak at 1100 cm^{-1} is due to asymmetric and symmetric stretching vibration of O=S=O group (from PEEK). The peak at 630cm^{-1} is assigned to S=O (from SPEEK). The prominent peak observed between 1600-1700 cm^{-1} is assigned to carbonyl group (C=O) of the ketone linked in PEEK chain. The broad peak observed between 1200-1600 cm^{-1} is due to the presence of C-H group (from PVA). Prominent peak observed between 3300-3450 cm^{-1} is assigned to O-H group from water and PVA. The peak intensity of the different function group is slightly shifted with each other for

different composites. It is observed that the peak intensity of different functional group (of PVA and SPEEK) decreased with increasing TiO_2 content.

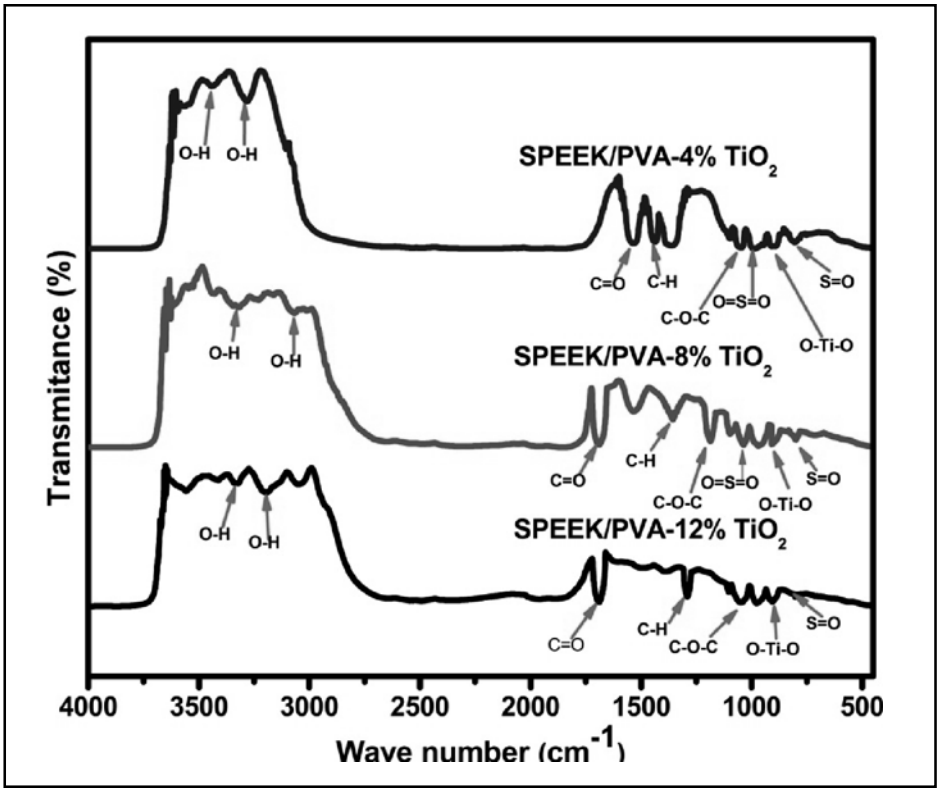

Fig. 2. FTIR spectra of the different TiO_2 loaded composite membrane.

X-ray diffraction of different composite membrane is shown in fig. 3. Low intensity peak is observed at various 2θ angles for SPEEK/PVA-4% TiO_2 membrane. The result indicates the semi crystalline structure with enriched amorphous region. The crystallinity of the composite is due to the addition of TiO_2 particle that diffracted the peak at some angle and existence of crystalline PVA. Further addition of TiO_2, membrane becomes more crystalline and degree of crystallinity of the composite rise. Enlarged crystalline phase of the material is observed for SPEEK/PVA- 8% TiO_2 composite. The enlargement of crystalline phase occurred in the composite due to the increase of degree of crystallinity (χ_c) of PVA. The crystalline region of PVA increased due to the nucleating ability of TiO_2 in PVA [40]. The more number of nucleation sites are formed and small crystal appeared. Further growth of the crystal occurred due to temperature gradient occurred in the composite. The addition of 4% TiO_2 in SPEEK/PVA, composite exhibits amorphous material. Further addition

of TiO_2 (8%), crystalline region of PVA increases and composite becomes lightly cross linked amorphous material. The crystalline region of PVA acts like a cross linking agent and membrane becomes ductile. Further addition of TiO_2 (12%) depleted amorphous region with enlarged crystalline phase resulting brittleness.

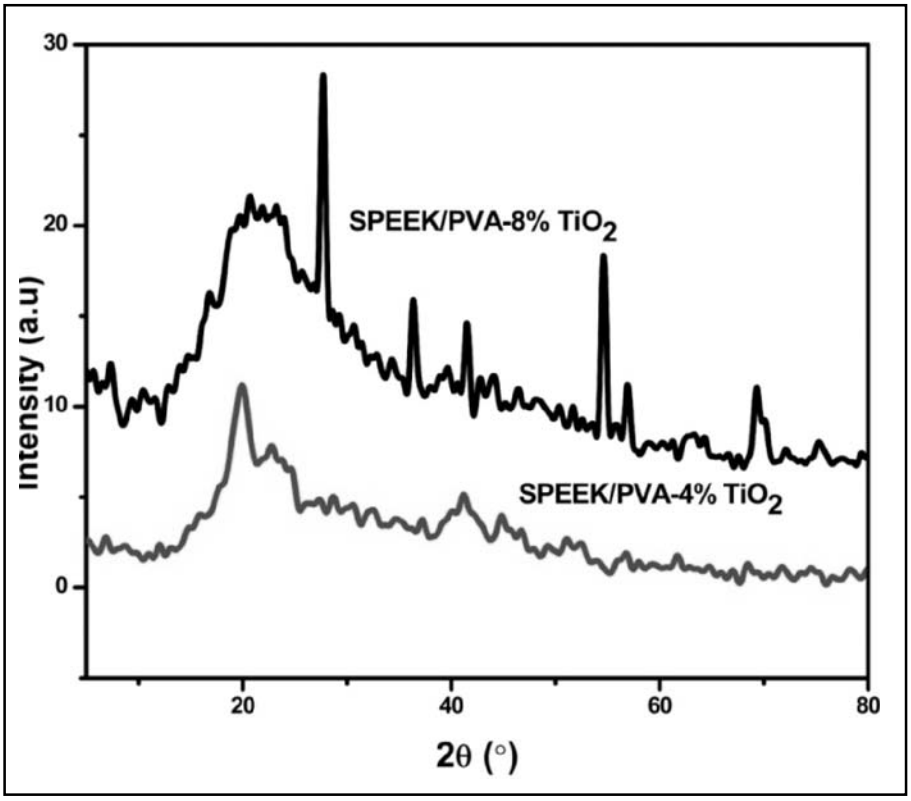

Fig. 3. X-ray diffraction of the different TiO_2 loaded composite membrane.

IEC and DS of the composite membranes are estimated by titration method. IEC, DS, WU (%) and λ values of the different composite membrane is shown in Table-1. IEC result indicates that with increasing TiO_2 content in the composite, IEC decreased. The reason for the reduction of IEC is due to the addition of TiO_2 which depleted effective area of ion transfer in the composite. Water uptake study reveals that water absorption capacity increased up to 8% TiO_2 loaded composite then drastically reduced. The drastic reduction of water absorption capacity is due to the cluster of TiO_2. It is found that addition of PVA in SPEEK resulting reduction of water absorption capacity. The reduction of water absorption capacity is due to its lower IEC and DS. But incorporation of TiO_2 in the SPEEK/PVA composite

enhancing water absorbing capacity due to the hygroscopic nature of TiO_2. The addition of TiO_2 creates free volume between TiO_2 and Polymer chain and hence water absorption capacity increased [40]. The value of λ at 90°C for different composite membrane is shown in Table-1. The increased of λ (Number of mol of H_2O absorbed per -SO_3H group) with TiO_2 content plays a major role for improvement of water absorption capacity. It is found that with addition of 8% TiO_2 in SPEEK/PVA composite, λ increased from 7 to 15. The water molecules absorbed on the TiO_2 surface are due to physical and chemical absorption. Chemically absorbed water molecules are weakly attached with each other by hydrogen bond, and the hydrogen atoms pointing towards bulk water. The water molecules absorbed by physical absorption are strongly bonded with each other with hydrogen atom pointing towards TiO_2 surface. The strong hydrogen bonding between physically absorbed water molecules via oxygen atoms of chemically absorbed molecules cause super hydrophilicity [41]. Due to its super hydrophilicity nature water absorption capacity of composites increased with increasing λ value. Further addition of TiO_2 content (12%) in SPEEK/PVA matrix, λ value decreased due to the formation of agglomeration or cluster creating free volume depletion resulting reduction of water absorption capacity. At 90°C, SPEEK/PVA-8% TiO_2 composite attained maximum value of λ due to strong hydrogen bonding between TiO_2 and water. But SPEEK membrane attained lower value of λ due to evaporation loss of water. Result indicates that SPEEK/PVA/TiO_2 composite membranes have higher water retention capacity than plain SPEEK and SPEEK/PVA membrane. The variation of λ with temperature is shown in fig. 4 (c). The λ value increased with temperature up to 85°C for all membrane and attained extreme for SPEEK/PVA-8% TiO_2 composite. Beyond 85°C, λ values drastically reduced for SPEEK and SPEEK/PVA membrane because of evaporation loss of water.

TABLE 1. Physical properties of different composite membranes.

Samples	IEC) (meqg^{-1})	DS (%)	WU (%)	λ (at 90°C)	Methanol Permeability (cm^2/sec.)×10^{-6}	Tensile Strength (MPa)	Modulus Elasticity, E (MPa)
SPEEK	1.93	69.20	48	9	32.43	58	1190
SPEEK/PVA	1.84	65.23	42	7	12.436	33	785
SPEEK/PVA-4% TiO_2	1.73	60.49	52	11	9.306	54	1542
SPEEK/PVA-8% TiO_2	1.64	56.72	64	15	3.703	66	1500
SPEEK/PVA-12% TiO_2	1.52	51.80	58	13	2.872	73	1921
Nafion (N115)	1.10		36		4.884	43	249
Nafion (N212)	0.7778		32		3.39	32	–
Nafion/Graphene Oxide (GO)[50]	0.55		12.9		1.017	62	1320

The variation of water uptake capacity (%) with temperature is shown in fig. 4(a). Water uptake capacity (%) is the important parameter of fuel cell that affects proton conductivity. Result indicates that the water absorption capacity of all membrane increased with temperature up to 85°C. Water absorption capacity enhanced with increasing temperature owing to the reduction of elastic modulus that results mobility of water molecule and enhancement of free volume between polymer chain [41, 42]. The improvement of water absorption by addition of TiO_2 is due to the reorientation of molecular structure with enhanced free volume. The variation of water absorption with time at higher temperature (90°C) is shown in fig. 4 (b). The rate of water absorption is very fast at the initial state of absorption process for all membrane. The rate of water absorption in SPEEK/PVA-TiO_2 composite is more than that of pure SPEEK due to the presence of water absorbing hygroscopic TiO_2 and higher water retention capacity. The variation of water diffusivity with temperature is shown in fig. 5. Water diffusivity result indicates that at low temperature, water diffusivity increased with increase in temperature for all membrane. It also indicates the variation of diffusivity in the order of 10^{-6} cm^2/sec. Incorporation of TiO_2 in a composite greatly affects water diffusivity. It is found that adding a small concentration (4%) of TiO_2 in SPEEK/PVA composite increases water diffusivity from $12\times10^{-6}cm^2$/sec for pure SPEEK/PVA to 32×10^{-6} cm^2/sec for SPEEK/PVA/TiO_2 composite. When the temperature rises above 80°C, water diffusivity drastically reduced for SPEEK and SPEEK/PVA membrane. The diffusivity data approaches lowest value of the order of $10^{-7}cm^2$/sec due to evaporation loss of water. But in case of SPEEK/PVA-TiO_2 composite, diffusivity data provides contrasting trend. The linear improvement of water diffusivity is observed with addition of TiO_2. The reason for improvement of water diffusivity is due to the formation of free volume between polymer chain, mobility of water molecule and improvement of λ values. The utmost diffusivity data is obtained for SPEEK/PVA-8% TiO_2 composite. Methanol permeability is crucial for designing effectively high performance fuel cell. Methanol permeability data is obtained from the glass diffusion cell and reported in Table-1. The study reveals that the TiO_2 has the significant effect on methanol permeability. By incorporating 4% TiO_2 in plain SPEEK/PVA matrix, methanol permeability reduced from 12.436×10^{-6} to 9.306×10^{-6} cm^2/ sec. Further addition of TiO_2 in SPEEK/PVA gradually reduced methanol permeability. The methanol permeability reduced with increasing TiO_2 in the SPEEK/PVA composite. The composite with 12% loaded TiO_2 shows lower permeability. The result shows that the methanol permeability of SPEEK/PVA-12% TiO_2 composite have lower than the N115 and N212 reported. The permeability result reported by S.J. Lue et. al. for Nafion/GO has slightly lower value than SPEEK/PVA-12% TiO_2 [50]. The methanol permeability result shows the good agreements with Nafion/GO membrane reported by Lue et. al. The reduction of methanol permeability improves fuel cell performance by minimizing fuel cross over across membrane electrode assembly.

The hydrolytic stability of the membrane plays important role for long term high humidity operation of fuel cell. In PEMFC, membrane with high water retention capacity performs better. The rate of loss of water at low humidity

environment for different composite membrane is shown in fig. 4 (d). The result indicates that water retention capacity of the composite increases with addition of TiO_2. The composite with 12 wt% loaded TiO_2 exhibits highest water retention capacity of 78% after long exposure time of 144 hours. The higher water retention capacity is attained because of the strong interaction between water and metal oxide preventing free escape of moisture due to evaporation. The SPEEK/PVA membrane showed least water retention capacity of 44% due to weak interaction between water and polymer backbone. Study reveals that TiO_2 loaded composite exhibits better hydrolytic stability.

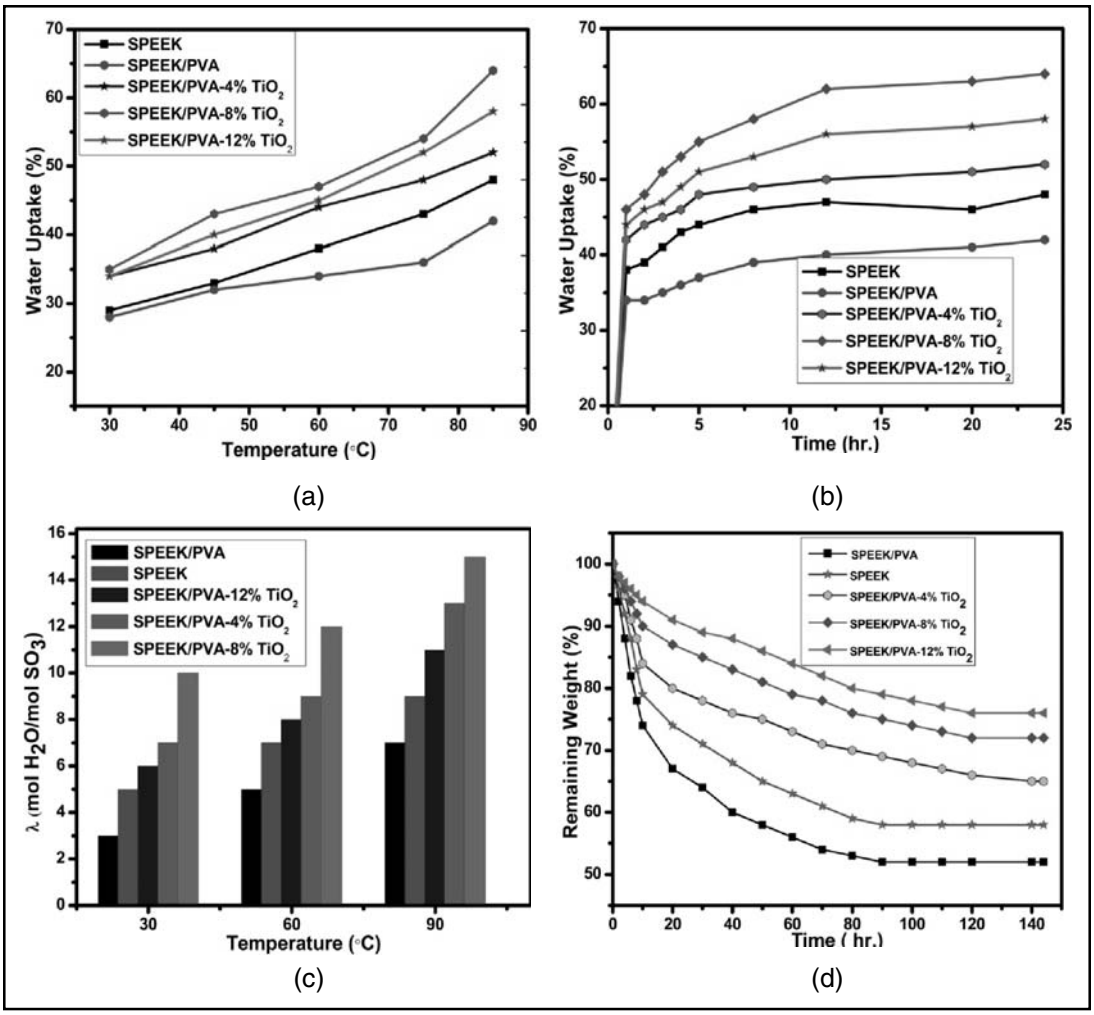

Fig. 4. Variation of moisture uptake for different composite membrane (a) with temperature (b) with time (c) Variation of λ with temperature (d) Variation of moisture loss with exposure time.

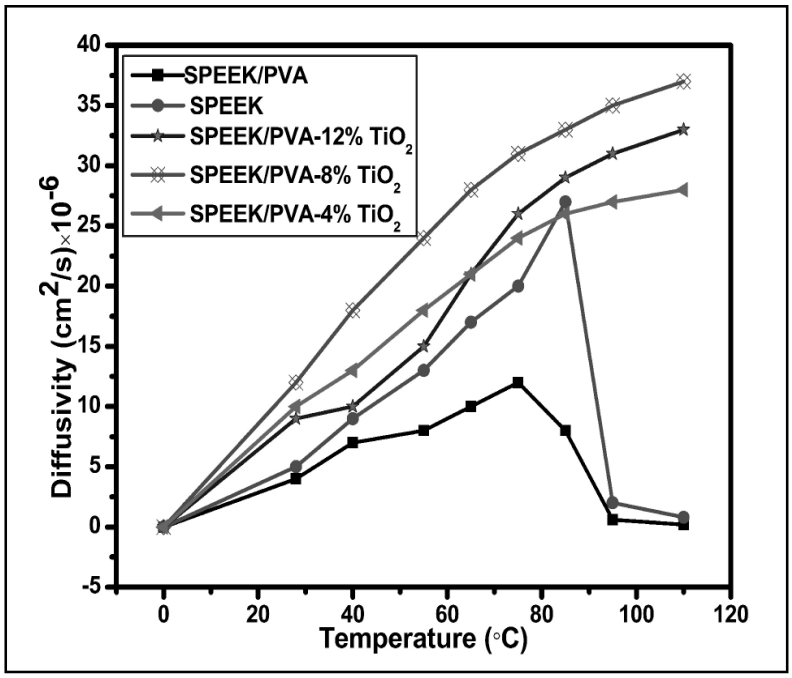

Fig. 5. Variation of water diffusivity with temperature for different composite membrane.

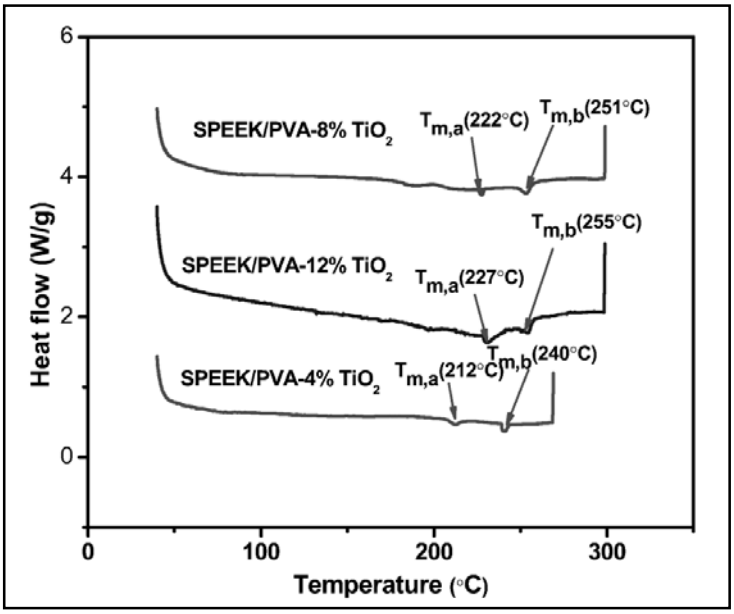

Fig. 6. Comparative DSC curve of different TiO_2 loaded composite membrane.

TABLE 2 : DSC results of the SPEEK composites.

Samples	T_g (°C)	$T_{m,a}$(°C)	$T_{m,b}$(°C)	ΔH_m^a (J/g)	χ_c^a (%)	T_c (°C)
SPEEK/PVA	135	160	185	12.20	29.25	176
SPEEK/PVA-4% TiO_2	170	212	240	14.88	35.68	198
SPEEK/PVA-8% TiO_2	182	222	251	17.16	41.15	236
SPEEK/PVA-12% TiO_2	204	227	255	19.92	47.76	228

The thermal and crystallization behavior of the SPEEK/PVA membrane is greatly influenced by TiO_2. The change of this behavior by action of heat is studied in DSC. At low temperature, SPEEK/PVA membrane behaves semi-crystalline nature with low melting and glass transition temperature. The glass transition temperature (T_g), melting temperature (T_m), heat of fusion and degree of crystallinity of different composite membrane obtained from DSC heating scan were shown in Table-2. Addition of PVA in SPEEK enhanced hydrophilic domain resulting weak intermolecular attraction between SPEEK and PVA and hence thereof reduction in glass transition temperature and melting temperature. But incorporation of TiO_2 in SPEEK/PVA matrix enhanced T_g and T_m. The crystallization temperature (T_c) is obtained from the exothermic peak of first cooling scan of DSC curve. The melting temperature is obtained in the endothermic peak of second heating scan. Study reveals that with addition of TiO_2 in a composites T_g, T_m, T_c and heat of fusion increases. The increment of T_g, T_m with different loading of TiO_2 content in composite membrane is shown in fig. 6. The composite membrane is obtained by the mixing of SPEEK, PVA and TiO_2. The material property of a particular component changes due to mixing. During mixing, the fundamental relation established between the material property (T_g, T_m ,T_c etc.) of SPEEK and PVA due to addition of TiO_2 is as follows

$$M_{i,j} = \frac{dM}{dx} \qquad (9)$$

Here i and j are denoted for SPEEK or PVA, M_i is the property of SPEEK or PVA after mixing, M is the property of SPEEK or PVA before mixing, x is the number of mole of TiO_2. M is expressed for T_g, T_m, T_c and heat of fusion of SPEEK and PVA. During mixing, material properties of SPEEK and PVA changes with addition of TiO_2. The decrease and increase of crystallization temperature is due to the effect of TiO_2 content and miscibility of the component. DSC result reveals the increment of T_g, T_m of SPEEK and PVA in a composite membrane due to addition of TiO_2. The improvement of glass transition temperature and melting temperate is due to the virtue of mixing effect and strong intermolecular attraction between TiO_2 and polymer backbone.

From DSC curve, $T_{m,a}$ and $T_{m,b}$ represents melting temperature of PVA and SPEEK respectively. Subscript a, b denotes polyvinyl alcohol and

SPEEK respectively. The degree of crystallinity (χ_c) of the PVA in a composite membrane is calculated by following equation

$$\chi_c^a(\%) = \frac{\Delta H_m^a}{\phi \Delta H_m^{o,a}} \quad (9)$$

χ_c^a is the degree of crystallinity of PVA in the composite membrane, $\Delta H_m{}^a$ is the heat of fusion (J/g) of PVA, $\Delta H_m{}^{0,a}$ is the heat of fusion (J/g) of 100% pure crystalline PVA. Φ is the weight fraction of PVA in a composite. For a 100% crystalline PVA, heat of fusion is 139 J/g[43]. The degree of crystallinity of PVA increases with increase of TiO_2 content. This is due to the fact that with addition of TiO_2, enhances rate of nucleation by forming supersaturate solution. With enriched degree of super saturation, large number of nuclei sites will form that resulted the increment of degree of crystallinity of PVA. It is worth noting that, TiO_2 has the significant effect on degree of crystallinity of PVA due to its nucleating ability.

Thermal stability of the composite membrane affects the performance of PEMFC. At low temperature, SPEEK membrane shows better

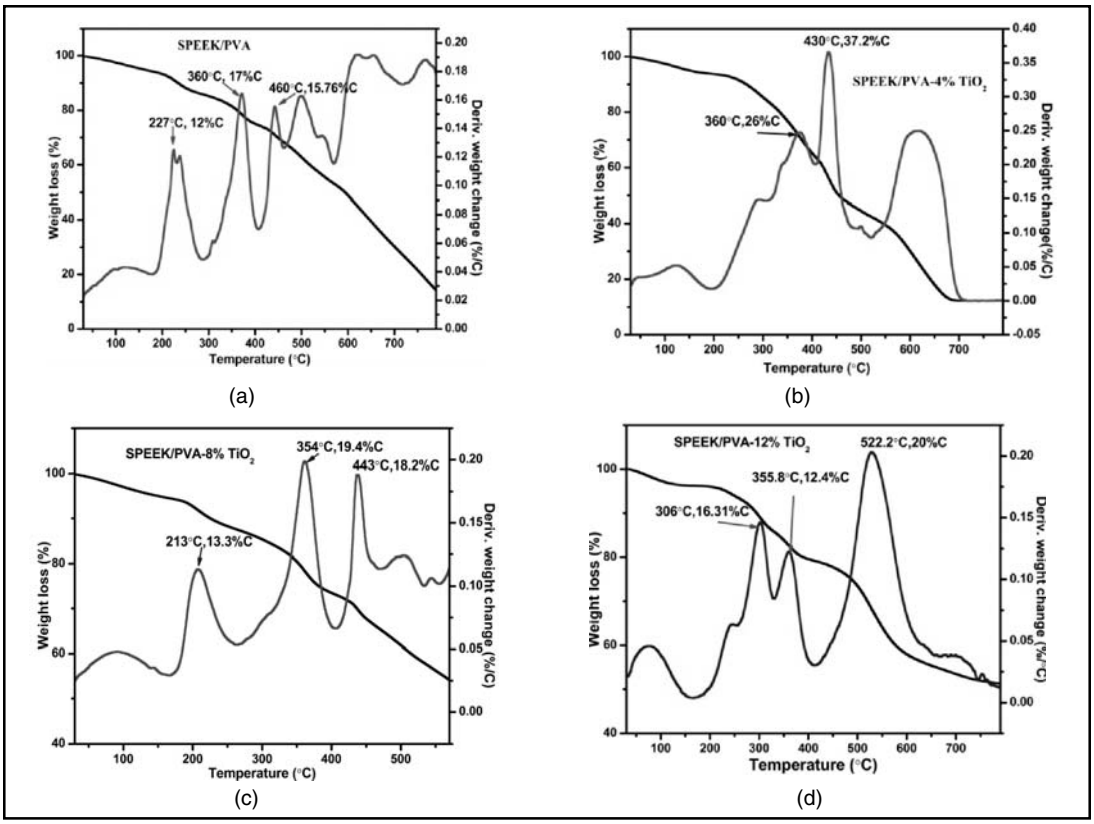

Fig. 7. TGA curve of (a) SPEEK/PVA membrane, (b) SPEEK/PVA-4% TiO_2, (c) SPEEK/PVA-8% TiO_2, (d) SPEEK/PVA-12% TiO_2

performance due to its high thermal stability. But at high temperature it accords low performance due to its poor thermal stability and degraded very fast. To improve its thermal stability at higher temperature, TiO_2 is incorporated in the SPEEK/PVA matrix. The TGA curve of different composite membrane is shown in fig. 7. The three major weight loss stages were observed for all composite membrane. The first weight loss is observed between 100-200°C due to loss of water by evaporation and residual solvent. When temperature exceeds the boiling point (165°C) of Dimethyl acetamide, vaporization started. The second weight loss stage is observed between 250-400°C due to thermal desulfonation of sulfonic acid group and degradation of PVA backbone. The third weight loss stage is observed between 650-800°C due to the thermal degradation of polymer backbone [44]. The thermal degradation of polymer backbone at higher temperature is due to the thermal oxidation of oxygen functional group such as carbonyl group. The maximum weight loss is observed at first weight loss stage due to the presence of more moisture content in the composite. During first weight loss stage, SPEEK/PVA membrane showed maximum weight loss due to the attachment of more sulfonate group in polymer backbone catalyzed degradation reaction [45]. The different weight loss stage of SPEEK/PVA membrane is shown in fig. 7(a). During first weight loss stage, with dispersion of 8% TiO_2 in SPEEK/PVA matrix, weight loss decreased from 12% to 7%, indicating the enhancement of thermal stability. During first weight loss stage, It is found that the thermal stability of the composite membrane increased with increasing TiO_2. The free radicals formed during thermal decomposition [46] will be captured by titanium dioxide, ensures the improvement of thermal stability. It is observed that in case of SPEEK/PVA, degradation of polymer backbone started

TABLE 3: Proton conductivity (S/cm) data of the different samples (Thickness: 120µm) measured by impedance analyzer at 30, 80 and 110°C.

Samples	Membrane Thickness (µm)	Proton 10^{-3} conductivity $(S/cm)^a \times 10^{-3}$	Proton Conductivity[1] $(S/cm)^b \times 10^{-1}$	Proton conductivity $(S/cm)^c \times 10^{-1}$
SPEEK	120	14.3	0.00059	0.00042
SPEEK/PVA	120	10.8	0.00032	0.00014
SPEEK/PVA-4% TiO_2	120	9.6	1.309	1.412
SPEEK/PVA-8% TiO_2	120	8.4	1.372	1.563
SPEEK/PVA-12% TiO_2	120	6.3	1.201	1.326
Nafion (N115)	120	77	2.3	
Nafion (N212)	50.8	78	3.8	
Nafion/GO (N212)	80	68	11.4	

Here superscript, a, b and c are the conductivity data reported at 30, 80 and 110°C respectively.

above 200°C due to thermal oxidation, resulted more weight loss than SPEEK/PVA/TiO_2 composite. But presence of TiO_2 in polymer backbone resists thermal degradation due to strong intermolecular attraction between TiO_2 and polymer chain. The major weight loss of SPEEK/PVA/TiO_2 composites due to thermal oxidation at more than 350°C is shown in fig. 7 (b, c, d). The rate of weight loss decreases with increase in TiO_2 content in the SPEEK/PVA matrix. The maximum weight loss (88%) is observed for SPEEK/PVA membrane with fewer residues. With addition of 8% TiO_2 in SPEEK/PVA, weight loss decreases from 88% to 22%. The addition of TiO_2 delays the deformation of oxygen functional group by creating interactive linkage between TiO_2 and polymer backbone. It is worth noting that increment TiO_2 from 8 to 12% exhibits minor improvement of weight loss. But it shifts the thermal oxidation of polymer backbone to higher temperature.

Proton conductivity is the important parameter affecting the performance of fuel cell. Electrochemical Impedance Spectroscopy (EIS) is a powerful technique to characterize

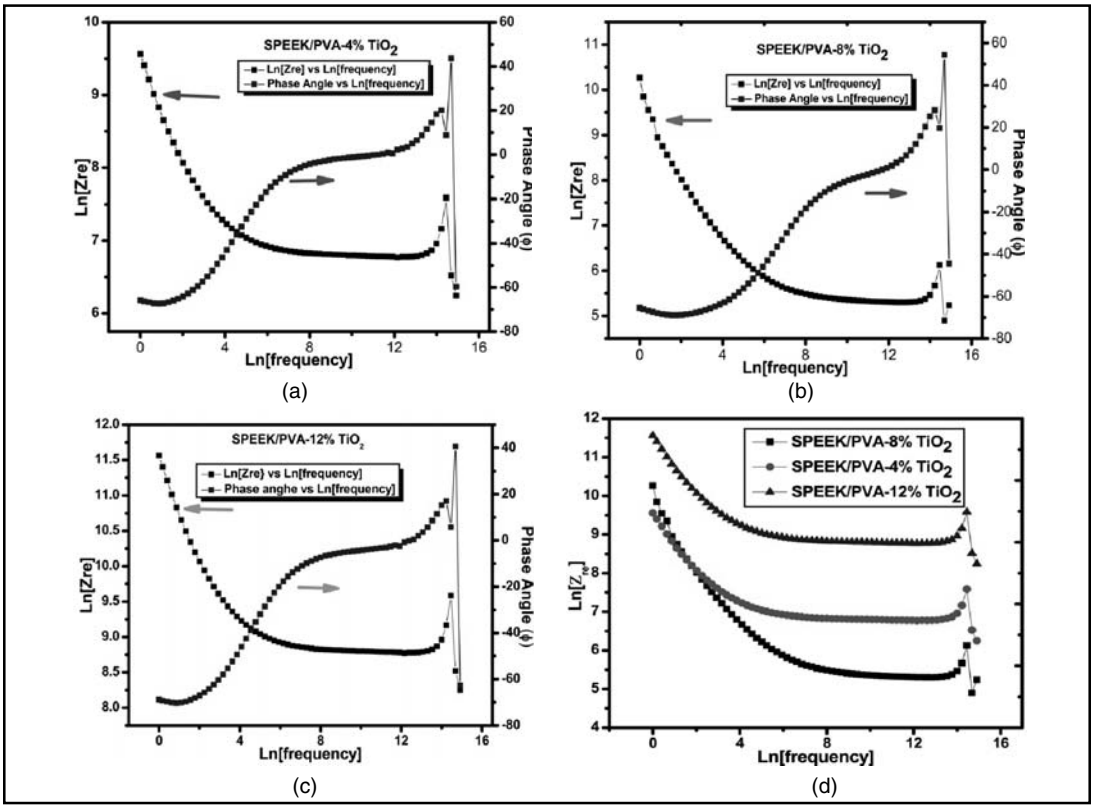

Fig. 8. Bode plot of composite membrane at 110°C for, (a) SPEEK/PVA-4% TiO_2, (b) SPEEK/PVA-8% TiO_2 (c) SPEEK/PVA-12% TiO_2, (d) Variation of membrane bulk resistance with frequency for different TiO_2 loaded composite membrane.

electrochemical system for measurement of impedance (Z) with wide range of frequency [47]. The variation of impedance and phase angle (ϕ) with frequency is observed. The bulk resistivity (R_b) of the membrane is obtained from the relationship between Z, f and ϕ by using two methods; (1) Bode diagram and (2) Nyquist plot. Bulk resistivity (R_b) determined from Bode plot and Nyquist plot; substituted in equation-8, yield Proton conductivity. Bode plot is one of the most convenient method for determining bulk resistivity (R_b). The dependence of impedance and phase angle with frequency for different composite membrane at 110°C is shown in fig. 8. From the log-log plot of impedance and frequency, R_b is obtained on the low intersect of high frequency region where phase angle reaches minimum. The variation of R_b with frequency for a different composite membrane is shown in fig. 8 (d). The bulk resistivity decreases with increase in frequency. The decrease and increase of bulk resistivity of different composite membrane is due to the presence of TiO_2.The addition of TiO_2 has the greatest effect on bulk resistivity. SPEEK/PVA-8% TiO_2 composite has the lowest bulk resistivity due to its better water retention capacity and enhancement of free volume. But further increase of TiO_2 i.e. for SPEEK/PVA/TiO_2, bulk resistivity increased resulting poor proton conductivity. This is due to formation of agglomeration emerge reduction in free volume between TiO_2 and polymer chain.

For Nyquist plot, real and imaginary part of impedance is plotted as shown in fig. 9 (a). The bulk resistivity of membrane decreased with increasing TiO_2 content. Proton conductivity of the different composite membrane with frequency is plotted in fig. 9 (b). The dispersion of TiO_2 has the greatest effect on proton conductivity. Proton conductivity increases with increase in frequency and its value is highest for SPEEK/PVA-8% TiO_2. For SPEEK/PVA-4% TiO_2 composite, proton conductivity increases with frequency. But further addition

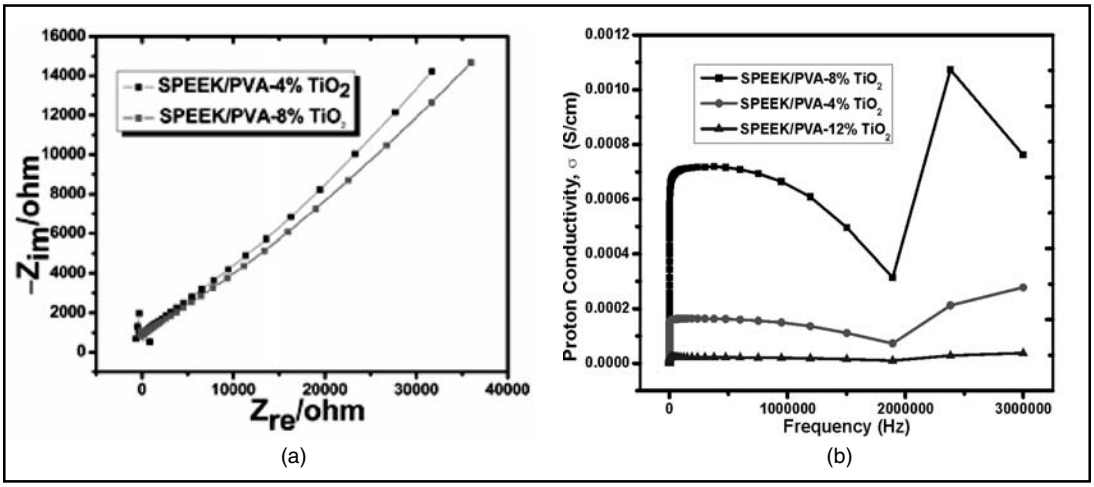

Fig. 9: Proton conductivity data of different TiO_2 loaded composite at 110°C (a) Nyquist plot (b) Variation of proton conductivity data with frequency.

of TiO_2, proton conductivity suddenly increased at low frequency then decreases in the lower to medium range frequency and it approaches utmost value at higher frequency. The decrease and increase of proton conductivity with frequency is due to the creation of some defects by dispersion of TiO_2. In EIS, proton conductivity is obtained in the high frequency region of impedance data. Proton conductivity measured at different temperature is summarized in Table-3. At lower temperature, IEC and DS have the greatest effect on proton conductivity. Due to higher DS 69.20% of SPEEK, it provides proton conductivity of 1.43×10^{-4} S/cm. Addition of PVA and TiO_2 in SPEEK decreases DS and hence proton conductivity decreases. SPEEK/PVA-12% TiO_2 composite membrane with DS 51.80% provides poor proton conductivity of 0.63×10^{-4} S/cm. At 110°C, TiO_2 has the significant effect on proton conductivity. Proton conductivity result reveals that with addition of TiO_2 in SPEEK/PVA matrix at 110°C improves proton conductivity. By incorporating 8% TiO_2 in SPEEK/PVA matrix, proton conductivity increased from 0.84×10^{-4} S/cm to 1.563×10^{-1} S/cm. Improvement of proton conductivity at higher temperature is accomplished by increment of λ values due to free volume enhancement with excellent water retention capacity and increment of proton transport mobility. But proton conductivity of SPEEK and SPEEK/PVA shows opposite trend. Proton conductivity data drastically reduced due to evaporation loss of water resulting poor water retention capacity. Proton conductivity of the SPEEK composite is compared with Nafion based composite reported by several researcher. The proton conductivity of the Nafion based composites is shown in Table 3. At 30°C temperature SPEEK composite provide lower proton conductivity than N115, N212 and Nafion/GO membrane. But at 80°C,

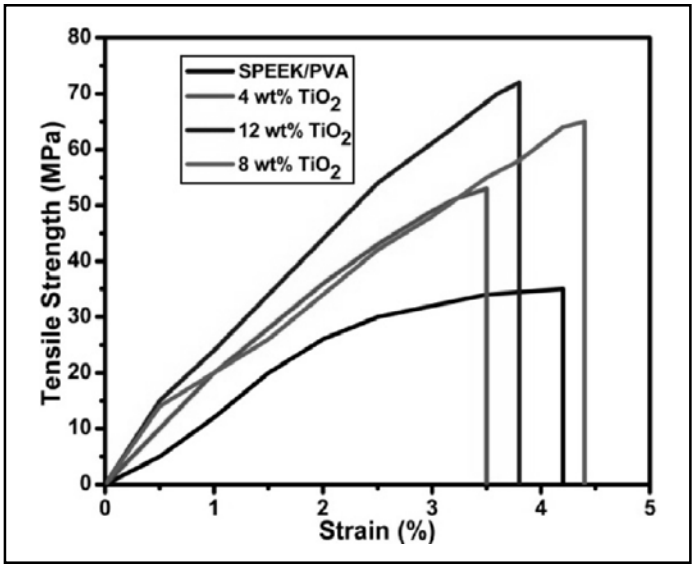

Fig. 10. Ultimate stress-strain curve for different composite membrane at 29°C and 60 % relative humidity.

remarkable increment of proton conductivity observed for SPEEK based composites with least variance than N115 and N212. Although it provides better proton conductivity but slightly lower than Nafion/GO membrane reported by Lue et. al.

The mechanical stability of the composite membrane plays an important role that affects fuel cell performance. The membrane with excellent mechanical stability has the interesting feature of longer life and ultimate tensile strength. During fuel cell operation, membrane with high mechanical stability performs better under different stresses for long duration of time. The different stresses involved in fuel cell are in homogeneous compression of electrode membrane assembly, mechanical shocks or transmitted vibrations and mechanical stresses from thermal hot spots [48]. The stress-strain behavior of different composite membrane is shown in fig. 10. From the stress-strain curve, tensile strength at break of the composite is evaluated. The modulus of elasticity (E) is obtained from the slope of the curve or the ratio between tensile strength and strain rate. The tensile strength and modulus of elasticity of different composite membrane is shown in Table-1. The result shows that the tensile strength increased with increasing TiO_2 content in SPEEK/PVA composite. The tensile strength of the composite is greatly affected by its orientation, degree of crystallinity and addition of TiO_2. SPEEK/PVA membrane is ductile in nature due to its hydrophilic nature. With increment of stress, strain rate linearly increases and membrane becomes more ductile. The increment of tensile strength due to addition of TiO_2 is because of the strong intermolecular interaction (i.e. hydrogen bonding and electrostatic forces) between polymer backbone and TiO_2 [49]. The other key factor related for enhancing tensile strength is cross linking. The composite behave like a lightly cross linked amorphous material. The present of crystalline region acts like a cross linking agent. Due to cross linked structure, tensile strength increased and composite becomes brittle. Maximum tensile strength (73 MPa) is obtained for SPEEK/PVA-12% TiO_2. But it has achieved lower strain rate than SPEEK/PVA membrane. The decrease in strain rate is due to its brittleness. The modulus of elasticity increased with increasing TiO_2 content and the composite becomes stiffer. The tensile strength of SPEEK/PVA-12% shows higher than Nafion/GO composite reported by S.J. Lue et.al.[50]. The SPEEK/PVA-8% TiO_2 provides reasonable tensile strength (66 MPA) with higher strain rate resulting ductility. The experimental result shows 33.73% increment of tensile strength by increasing TiO_2 from 4% to 12% in SPEEK/PVA matrix.

5. CONCLUSION

Our experimental work features some remarkable conclusions. The developed SPEEK/PVA/TiO_2 composite membrane possesses higher mechanical strength, better thermal stability and proton conductivity. The prepared composite membrane can be applicable in higher temperatures at 110°C. The prepared composite membrane shows lower methanol permeability due to the reduction of void volume between polymer chain interfaces. The improvement of proton conductivity of the composite membrane is by the virtue of strong intermolecular attraction (Hydrogen bonding) between TiO_2 and water,

thereby improves the water retention capacity and the super hydrophilicity. At low to medium temperature, IEC and DS have moderate effect on proton conductivity. But at higher temperature, TiO_2 has the significant effect on proton conductivity. The reason behind the superior mechanical strength is due to the development of cross linked semi crystalline structure. It is noteworthy to conclude that, the prepared composite membrane with 8% TiO_2 shows the optimized performance. At higher temperature (above 85°C), lightly cross linked SPEEK/PVA/TiO_2 composite membrane could be considered as potential candidate in PEMFC. A further extension of the above research work may be implemented by studying the performance of the composite membrane in PEMFC.

REFERENCES

1. Papageorgopoulous D.(2010), DOE fuel cell technology program overview and introduction to the 2010 fuel cell pre-solicitation workshop in DOE fuel cell pre-solicitation workshop, Department of Energy, Lakewood, Colorado.
2. I, Colicchio, DA, Demco, M, Baias, H, Keul, H. Moeller. (2009), *Journal of Membrane Science,* 337, 125-135.
3. H. W. Zhang and P. K. Shen (2012) *Chemical Reviews,* 112 (5), 2780–2832.
4. S. Zhong, X. Cui, H. Cai, T. Fu, C. Zhao and H. Na, (2007). *Journal of Power Sources,* 164, 65–72.
5. S. J. Peighambardoust, S. Rowshanzamira and M. Amjadi, (2010). *International Journal of Hydrogen Energy,* 35 (17), 9349–9384.
6. A. Kraytsberg and Y. Ein-Eli, (2014). *Energy & Fuels,* 28 (12), 7303–7330.
7. B. C. H. Steele and A. Heinzel, *Nature,* 414 (6861), 345–352.
8. S. Subianto, M. Pica, M. Casciola, P. Cojocaru, L. Merlo, G. Hards, *Journal of Power Sources,* 2013, 233, 216-30.
9. E. Sgreccia, M. Di Vona, S. Licoccia, M. Sganappa, M. Casciola, J. Chailan, P. Knauth. *Journal of power Sources,* 2009, 192, p:353-359.
10. H. Do gan, TY Inan, E Unveren, M. Kaya. (2010). *International Journal of hydrogen energy,* 35, 7784-95.
11. P. X. Xing, G. P. Robertson, M. D. Guiver, S. D. Mikhailenko, K. P. Wang, S. Kaliaguine, (2004) . *Journal of Membrane Science,* 229, 95-106.
12. J. Jaafar, A. F. Ismail, A. Mustafa, (2007). *Material Science and Engineering: A,* 460, 475-484
13. S. M. J. Zaidi, S. D. Mikhailenko, G. P. Robertson, M. D. Guiver, S. Kaliaguine, *Journal of Membrane Science,* 2000, 173, 17.
14. B. Bauer, D. J. Jones, J. Roziere, L. Tchicaya, G. Alberti, M. Casciola, L. Massinelli, A. Peraio, S. Besse, E. Ramunni. (2000). *Journal of New Materials for Electrochemical System,* 2000, 3, 93.
15. D. X. Luu, E. B. Cho, O. H. Han, D. Kim. (2009) *Journalof Physical Chemistry B.,*113 (30) 10059-62,
16. E. Sengul, H. Erdener, R. G. Akay, H. Yucel, N. Bac and I. Eroglu. (2009). *International Journal of Hydrogen Energy,* 34, 4645–4652.
17. C Gong, X Zheng, H Liu, G Wang, F Cheng, G Zheng. (2016). *Journal of Power Sources,* 325, 453-64.
18. VR Hande, S Rao, S Rath, A Thakur, M Patri. (2008) *Journal of Membrane Science,* 322, 67-73.
19. S Han, M-S Zhang , J Shin, Y-SLee. (2014) 1, 6-Bis (4-vinylphenyl) hexane as a crosslinking agent for the preparation of cross linked sulfonated poly (ether ether ketone) membranes by EB irradiation. 97, 313-8.

20. J-M Song, DW Shin, J-Y Sohn, YC Nho, YM Lee, J Shin. (2013). *Journal of Membrane Science,* 430, 87-95.

21. AG Lafi Al, JN Hay. (2015) *Thermochimica Acta,* 612, 63-9.

22. N Ramly, N Aini, N Sahli, S Aminuddin, M Yahya, A Ali. (2016). *International Journal of Hydrogen Energy,* 42 (14).

23. PR Jothi, S Dharmalingam. (2014). *Journal of Membrane Science* 450, 389-96.

24. J. W. Rhim, H. B. Park, C. S. Lee, J. H. Jun, D Kim, Lee S., Y. M. Lee. (2004). *Journal of Membrane Science,* 238, 143.

25. N.W. DeLuca, Y.A. Elabd. (2006). *Journal of Power Sources,* 163, 386–391.

26. Z.-G. Shao, X. Wang, I.M. Hsing, (2002). *Journal of Membrane Science,* 210, 147–153.

27. Sergio Molláab, Vicente Compan. (2011). *Journal of membrane science,* 372, 191-200.

28. P. Kanakasabai, P. Deshpande Abhijit, Susy Varughese. (2013). *Journal of Applied polymer science,* 127 (3), 2140-2151.

29. Chun-Chen Yang. (2007). *Journal of membrane science,* 288, 51-60.

30. Du L, Yan X, He G, Wu X, Hu Z, Wang Y. (2012) SPEEK proton exchange membranes modified with silica sulfuric acid nanoparticles. *InternationalJournal of Hydrogen Energy* 37, 11853-61.

31. J Wang, H Bai, H Zhang, L Zhao, H Chen, Y Li. (2015). *Electrochimica Acta,* 152, 443-55.

32. D Gupta, A Madhukar, V Choudhary. (2013). *InternationalJournal of Hydrogen Energy,* 38, 12817-29.

33. V, Baglio, A.S. Arico, A.D. Blasi, V. Antonucci, P.L. Antonucci, S. Licoccia, E. Traversa, F.S. Fiory. (2005). *Electrochimica Acta* 50 (2005) 1241-46.

34. S. Panero, P. Fiorenza, M.A. Navarra, J. Romanowska, B.Scrosati (2005). *Journal of Electrochemical Society* 152 (12).

35. Gashoul Fatemeh, Parnian Mohammad Javad, Rowshanzamir Soosan (2017). *International journal of hydrogen energy,* 42, 590-602.

36. Qiu Xiang, Dong Tiandu, Ueda Mitsuru, Zhang Xuan, Wang Lianjun (2017). *Journal of membrane science,* 524, 663-672.

37. R. Murmu, H. Sutar. (2018). *Journal of polymer materials,* 35 (1), 103-118.

38. T. Takamatsu, M. Hashiyama, A. Eisenberg. (1979). *Journal of Applied Polymer Science* 24 (11) (1979) 2199–2220.

39. D.R. Morris, X.D. Sun. (1993). *Journal of Applied Polymer Science,*50 (8), 1445–1452.

40. Chun-Chen, Yang. (2007). *Journal of membrane science,* 288, 51-60.

41. Saman Hosseinpour, Fuie Tang, Fenglong Wang, A. Livingstone Ruth, J. Schlegel, OhtoTatsuhiko, Mischa Bonn, Yuki Nagata and H. Backus Ellen G. (2017). *The Journal of Physical Chemistry Letters,* 8, 2195-2199.

42. H Zhang, C Ma, J Wang, X Wang, H Bai, J Liu. (2014). *International Journal of Hydrogen Energy*, 39, 974-86.

43. M. S. Peresin, Y. Habibi, J. O. Zoppe, J. J. Pawlak and O. J. Rojas (2010). *Bio macromolecules,* 11, 674–681.

44. D. S. Kim, H. B. Park, J. W. Rhim, Y. M. Lee. (2005). *Solid State Ionics,* 176, 117-126.

45. P Xing, GP Robertson, MDGuiver, SD Mikhailenko, K Wang, S Kaliaguine. (2004). *Journal of Membrane Science,* 229, 95-106.

46. G. Gonçalves, AAP MarquesPaula, Barros-Timmons Ana, Igor Bdkin, M. K. Singh, N. Emami and J. Gracio. (2010). *Journal of material chemistry,* 20 (44), 9927–9934.

47. E. P. Randviir and C. E. Banks (2013). *Analytical Methods,* 5, 1098–1115.

48. MF Serincan, U. Pasaogullari. (2011). *Journal Power Sources,* Vol.196, 1303-13.Wu H,

49. Y Cao, Z Li, G He, Z Jiang. (2015). *J Power Sources,* 273, 544-53.

50. Lue Shingjiang Jessie, Pai Yu-Li, Shih Chao-Ming, Wu Ming-Chung, Lai Sun-Mou. (2015). *Journal of Membrane Science,* 493,212-223.

Received: 12-11-2018

Accepted: 25-01-2019